Journal of Applied Polymer Science

MWNT-Filled PC/ABS Blends: Correlation of Morphology with Rheological and Electrical Response

Seyedali Monemian,[1,2] Seyed Hassan Jafari,[1] Hossein Ali Khonakdar,[3] Vahabodin Goodarzi,[1] Uta Reuter,[4] Petra Pötschke[4]

[1]School of Chemical Engineering, College of Engineering, University of Tehran, Tehran, Iran
[2]Department of Macromolecular Science and Engineering, Case Western Reserve University, Cleveland, Ohio 44106-7202
[3]Department of Polymer Processing, Iran Polymer and Petrochemical Institute, Tehran, Iran
[4]Leibniz Institute of Polymer Research Dresden, Hohe St. 6, D-01069, Dresden, Germany
Correspondence to: S. H. Jafari (E-mail: shjafari@ut.ac.ir)

ABSTRACT: A systematic study was done on morphological, electrical and rheological behavior of co-continuous or dispersed-type polycarbonate (PC)/acrylonitrile-styrene-butadiene (ABS) blends, containing different amounts of multiwalled carbon nanotubes (MWNT). The MWNTs gave substantial electrical conductivities to these nanocomposites at very low concentrations, owing to the effective melt processing method. Because of selective localization of MWNTs in the PC phase, along with double percolation phenomenon, the blend with co-continuous morphology showed a lower electrical and rheological percolation threshold, higher melt viscosity and elasticity, as compared to the system with dispersed morphology. The morphology of both the blend systems was refined as a result of MWNTs incorporation but the morphology type remained unchanged. A typical role of compatibilizer in refining blend morphology was observed in both the systems. The electrical conductivity of the system filled with MWNTs in presence of compatibilizer, was lower than the systems filled with MWNTs only, which was attributed to role of compatibilizer in directing a part of MWNTs from PC matrix toward ABS phase. With increasing compatibilizer/MWNTs ratio, the influence of compatibilizer on morphology refinement and conductivity reduction was intensified. By comparing TEM micrograph of PC/SAN/MWNTs with that of PC/ABS/MWNTs, it was revealed that small portion of MWNTs was also located on polybutadiene rubber fraction of ABS. © 2013 Wiley Periodicals, Inc. J. Appl. Polym. Sci. 000: 000–000, 2013

KEYWORDS: blends; morphology; nanotubes; graphene and fullerenes; polycarbonates

Received 5 January 2013; accepted 23 February 2013; published online
DOI: 10.1002/app.39211

INTRODUCTION

Since the first patent on multiwalled carbon nanotubes was filed in 1987,[1] and Iijima first detailed paper showing high resolution TEM of carbon nanotubes (CNT) in 1991,[2] considerable interest has been drawn on CNT-based polymer nanocomposites, due to their unique mechanical and electrical properties.[3] Although many high strength and electronically conductive CNT-filled polymer nanocomposites have been prepared to date, comparably little work has been carried out on nanocomposites based on polymer blend systems.[4–12] Polymer blend nanocomposites may lead to a new class of high performance materials, which combine the advantages of polymer blends and the merits of polymer nanocomposites. The properties of CNT-filled polymer systems are highly influenced by the nanofiller content, as well as its morphological state. The electrical conductivity of these materials discontinuously increases with CNT content. At certain concentration, a sudden change in the morphological state of the conductive tubes occurs, which is called "percolation threshold." At this concentration, a CNT network is formed by interconnected nanotubes.[13,14] Through efficient dispersing of primary nanotube agglomerates, a higher amount of tubes would be available to form the percolated network. In blend based nanocomposites, the amount of tubes needed to reach electrical percolation can be even lower than that of a single-polymer composite, if the nanotubes selectively localize in a continuous phase or at the interface. Especially desired are co-continuous blends, where a double percolation phenomenon can be achieved. The percolation threshold is then dependent on the amount of CNT, and also on the blend morphology, which in turn is a function of blend composition, the compatibilizer, and the processing conditions. For a system similar to the commercially important PC/ABS system under investigation

in this study, selective localization and migration of MWNTs toward the PC phase in PC/SAN blends, even if the nanotubes were first dispersed in SAN, have been reported before.[11] It was shown that this selective localization has led to lower electrical percolation threshold in the blends as compared to the single-polymer nanocomposites.

Dynamic rheological measurements are shown to be a suitable tool to evaluate material structure without destruction of the structure under investigation. On the one hand, the rheological properties of the molten components in immiscible polymer blends affect the blend morphology, and thus, the processing/morphology/property relationships. Moreover, from rheological measurements it is possible to deduce on the morphology of multiphase blends.[15] The addition of nanofiller changes the rheological properties of the filled component(s), and thus, may also change the developed blend morphology. It has been found that a characteristic viscoelastic response reflects the development of a combined polymer-nanotube network structure, which can be attributed to a rheological percolation.[16,17]

In immiscible polymer systems, it is necessary to modify the interface between the polymer blend phases by compatibilization that induces a better adhesion and a lower interfacial tension between the phases, and results in uniform and a refined morphology of the dispersed phase. On the other hand, a compatibilization between the nanotubes and the polymer phase(s) can be useful to positively affect the state of filler dispersion, and adhesion between nanotubes and polymer.[18]

In case of polymer-nanotube composites with single polymer matrix, the interrelationships between electrical, morphological, and rheological properties have been studied intensively over the last decade.[19–22] However, these relationships have been rarely studied in the same extent for immiscible polymer blend-based nanocomposites.

In this article, a systematic investigation is presented that characterizes melt processed polycarbonate (PC)/acrylonitrile butadiene styrene copolymer (ABS)/MWNT nanocomposites by varying the nanofiller content, and filler to compatibilizer ratio, at two fixed blend compositions. A styrene-acrylonitrile-maleic anhydride copolymer (SAN-MA) is used as compatibilizer to mediate between the blend components, and also possibly, to direct CNTs toward ABS phase. The strong polar nature of MA group and its affinity toward CNTs, together with interaction between the common SAN phases of the compatibilizer and ABS can induce a coupling between CNTs and ABS.

This study combines morphological investigations on blend morphology and filler dispersion with electrical and rheological characterization. Immiscible PC/ABS blends are well established commercial materials having a good combination of toughness, stiffness, and processability.[23] Considering the role of CNTs in enhancement of electrical performances of polymers, it is expected that the addition of small amount of multiwalled carbon nanotubes (MWNTs) to the PC/ABS blend system improves its electrical properties without impeding its processability.

EXPERIMENTAL

Materials

All materials (T45 Bay Blend, T85 Bay Blend, Polycarbonate Macrolon 2600, SAN Lustran M60, ABS Novodour Graft (SAN-g-PB) and SAN-MA) were supplied by Bayer AG. T45 is a commercial PC/ABS blend (ABS-rich). It is a general purpose injection molding grade with melt volume flow-rate (MVR) of 12 cm^3/10 min (at 260 °C, 5 kg), and melt viscosity of 200 Pas (at 260°C, 1000 s^{-1}). T85 is a high impact PC-rich blend with a MVR of 12 cm^3/10 min and melt viscosity of 290 Pas. The MWNTs employed in this work were Nanocyl™ NC 7000 (Nanocyl S.A., Sambreville, Belgium), an as produced material with a carbon purity >90% with average tube length of 1.5 μm and average diameter of 9.5 nm. Before mixing, the polymers and MWNT were dried in a vacuum oven at 100 °C for 4 h.

Sample Preparation

The nanocomposites were prepared through a one-step process in a small scale DACA Microcompounder (conical twin screw compounder with 4.5 cm^3 capacity). Prior to the melt mixing process, the commercial blends were dry-premixed with MWNT in a specified ratio, and then, fed into the compounder. The detailed composition of the studied samples is presented in Table I. A processing temperature of 260°C, a screw speed of 150 rpm, and a mixing time of 5 min were used for preparation of the blends and nanocomposites. The extruded strands were cooled on an aluminum tray in air. For electrical conductivity studies, the extruded strands were compression molded into rectangular 0.5-mm thick sheets with dimensions of 20 × 10 mm^2 at 260°C and 10 MPa.

Characterization

The dispersion of the MWNTs in the blend was studied by means of transmission electron microscopy (TEM). Ultra thin sections of the extruded samples (approximately 70-nm thick) were obtained at room temperature, using an EM UC/F6 ultramicrotome equipped with a diamond knife. The cuts were observed by means of a Leo 910 (Carl Zeiss) microscope using an accelerated voltage of 120 KV.

Scanning electron microscopy (SEM) was used to characterize the morphology of the blends and nanocomposites. An extruded polymer strand was immersed in liquid nitrogen for some time, and a brittle fracture was performed. The fractured surface for ABS-rich samples (T45) was etched in NaOH solution, capable of hydrolyzing PC phase only, at 105°C for 45 min. Also, the fractured surface for PC-rich samples (T85) was etched in sulfochromic acid solution, capable of oxidizing only ABS or SAN phase at 80°C for 15 min. The etched surfaces were placed in hot water at 80°C for 20 min. After proper drying, they were gold sputtered and observed under a PHILIPS CM200.

For determination of electrical properties of the samples having lower electrical conductivity (electrical resistivity higher than 10^7 Ω cm^{-1}), thin sheets with 60 mm diameter and 0.35 mm thickness were prepared by compression molding at 260°C and 10 MPa, and electrical volume conductivity was measured using an electrometer model 6517 combined with a 8009A Resistivity Test Fixture (both from Keithley). In the case of samples with higher electrical conductivity (electrical resistivity lower than

Table I. Composition of Studied Samples

Sample code	PC (wt %)	SAN (wt %)	ABS (wt %)	SANMA (wt %)	MWNTs (wt %)
PC	100	–	–	–	–
SAN	–	100	–	–	–
ABS	–	–	100	–	–
PC/CNT0.75	97.25	–	–	–	0.75
SAN/CNT0.75	–	97.25	–	–	0.75
ABS/CNT0.75	–	–	97.25	–	0.75
T45	45	–	55	–	–
T85	70	–	30	–	–
T45C0.05	–	–	–	–	T45+0.05
T45C0.1	–	–	–	–	T45+ 0.1
T45C0.25	–	–	–	–	T45+0.25
T45C0.5	–	–	–	–	T45+0.5
T45C1	–	–	–	–	T45+1
T85C0.05	–	–	–	–	T85+0.05
T85C0.1	–	–	–	–	T85+0.1
T85C0.25	–	–	–	–	T85+0.25
T85C0.5	–	–	–	–	T85+0.5
T85C1	–	–	–	–	T85+1
T45S0.5C0.5	–	–	–	T45 +0.5+0.5	
T45S2C0.5	–	–	–	T45+2+0.5	
T45S4C0.5	–	–	–	T45+4+0.5	
T85S0.5C0.5	–	–	–	T85+0.5+0.5	
T85S4C0.5	–	–	–	T85+4+0.5	
T45S2.5	–	–	–	T45+2.5	–
T45S4.5	–	–	–	T45+4.5	–
T85S4.5	–	–	–	T85+4.5	–
PC70/SAN30/SANMA0.75/CNT0.75	68.95	29.55	–	0.75	0.75
PC70/ABS30/SANMA0.75/CNT0.75	68.95	–	29.55	0.75	0.75

$10^7\ \Omega\ cm^{-1}$), strips with $20 \times 3 \times 0.5\ mm^3$ were cut from the pressed sheets and electrical conductivity was measured using Keithley model 2000 electrometer combined with a four-point test fixture having two gold wire electrodes in a distance of 16 mm and two measuring electrodes 10 mm apart. The reported values are average of at least four measurements for each sample.

Dynamic rheological characterization was performed in a MCR300 rheometer (Anton Paar) with a 25 mm parallel plate fixture and a gap of 0.5 mm at 260°C under nitrogen atmosphere. Frequency sweeps from 100 to 0.1 rad/s were carried out. Prior to the measurements, strain sweep tests were performed to determine the linear viscoelastic strain range. The samples for rheological test were cut from thin sheets with 60-mm diameter and 0.35-mm thickness, which were prepared by compression molding at 260°C and 10 MPa.

RESULTS AND DISCUSSION

Blend Morphology

Figure 1 shows SEM images of cut surfaces of the T45 (ABS-rich) blend and its nanocomposites, in which the PC phase was removed by hydrolization, and thus, appears in black. Although in some regions, large and deformed droplets are observable on the surface of the etched cuts of T45 blend [Figure 1(a)], it is observed that T45 morphology is close to the co-continuity window [inset image of Figure 1(a)]. Addition of 0.5 wt % MWNTs to this blend refines the PC phase [Figure 1(b)]. Addition of 1 wt % MWNTs further refines the co-continuous morphology [Figure 1(c)]. Incorporation of 4.5 wt % SAN-MA as compatibilizer into the pure T45 blend changes the co-continuous to a dispersed-type morphology [Figure 1(d)]. This can be attributed to reduction of interfacial tension of the system due to increased interfacial interactions between the blend components.[23] By simultaneous addition of 0.5 wt % SAN-MA and 0.5 wt % MWNTs to T45 blend, a coarsening of the co-continuous morphology of the T45 blend compared to that of noncompatibilized T45C0.5 nanocomposite sample was observed [comparing Figure 1(e) with 1(b)], though it has a finer co-continuous morphology as compared to the neat T45 sample [comparing Figure 1(e) with 1(a)]. As it was expected, the compatibilizer seems to be able to establish some sort of coupling between CNTs and ABS, which may help in directing CNTs from PC phase toward ABS phase. As a result of this, the slight

Applied Polymer SCIENCE

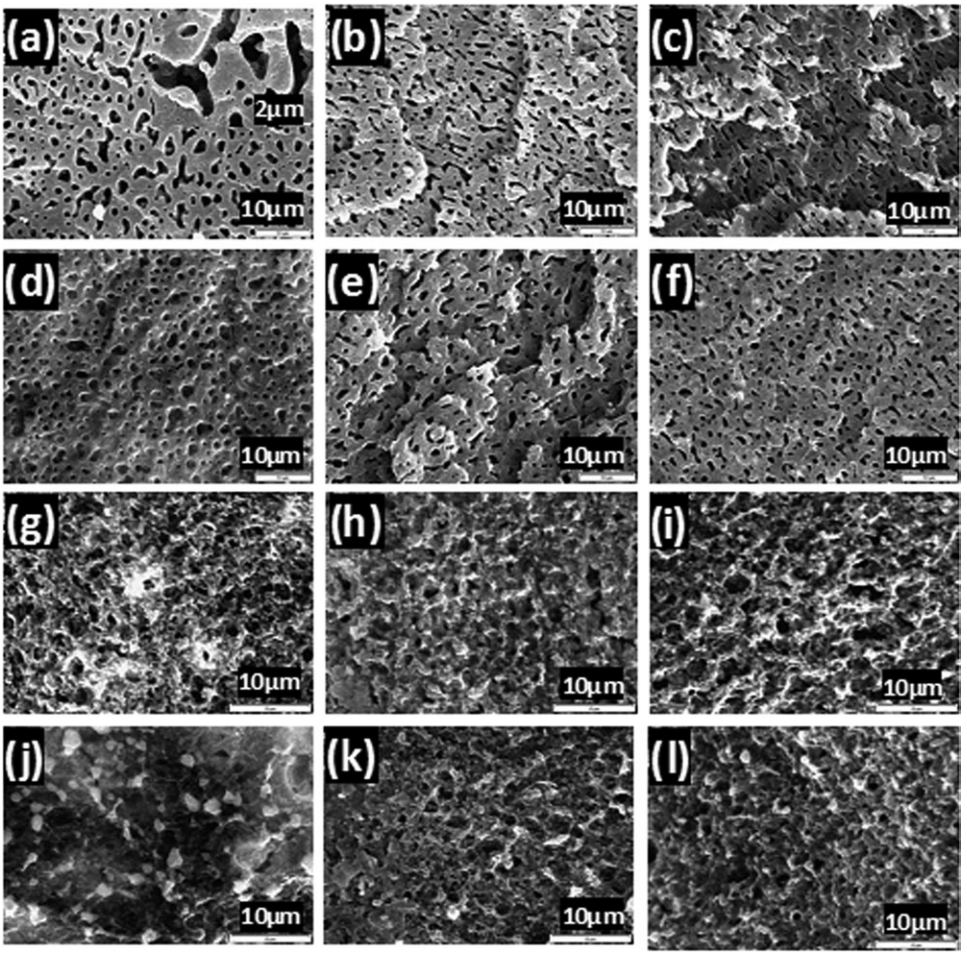

Figure 1. SEM images of T45 and T85 blends and the blend-based nanocomposites: (a) T45, (b) T45C0.5, (c) T45C1, (d) T45S4.5, (e) T45S0.5C0.5, (f) T45S4C0.5, (g) T85, (h) T85C0.5, (i) T85C1, (j) T85S4.5, (k) T85S0.5C0.5, and (l) T85S4C0.5 (For T45, PC etched out using NaOH, and for T85, ABS etched out using sulfochromic acid solution).

coarsening of PC phase is justifiable. Increase of SAN-MA/MWNT ratio from 1 to 8 refines the blend morphology again [comparing Figure 1(e) with 1(f)], which can be attributed to compatibilization role of SAN-MA. The higher amount of SAN-MA pronounces the interfacial interactions between the blend components, and this leads to morphology refinement.

Figure 1 also depicts SEM images of the PC-rich T85 blend and its nanocomposites. Generally, in these series of samples, clear morphologies are not seen. Here, the ABS and SAN phases of the blends have been etched out, and therefore, they appear as black dots dispersed within the remaining PC matrix. In a first look, large differences in the size of dispersed phase are not seen within these series of samples. The unmodified blend shows dispersed-type morphology [Figure 1(g)]. Addition of 0.5 wt % MWNTs to this blend decreases the size of dispersed phase droplets, slightly, and refines the morphology [Figure 1(h)]. The selective localization of MWNTs in PC matrix may increase its viscosity, which changes viscosity ratio, and therefore, smaller ABS droplets form. Addition of 1 wt % MWNTs further refines the morphology. Unlike the T45 system, addition of 4.5 wt % SAN-MA to the pure blend does not change the morphology type [comparing Figure 1(g) with 1(j)]. This could be due to the fact that the system is sufficiently far away from co-continuity region, and therefore, presence of compatibilizer is not capable of changing the general appearance of the dispersed-type morphology of the blend. Simultaneous addition of 0.5 wt % MWNTs and 0.5 wt % SAN-MA to T85 blend increases the size of droplets [Figure 1(k)], compared to that of noncompatibilized sample [Figure 1(h)]. As mentioned above, the reason can be attributed to the role of compatibilizer in directing MWNTs toward ABS phase. This increases viscosity and elasticity ratio of the system (dispersed phase to matrix), and hence, bigger droplets can be formed. Due to the same reason, an increase of SAN-MA/MWNTs ratio from 1 to 8 increases the size of droplets [comparing Figure 1(k) with 1(l)].

MWNT Dispersion State

Figure 2 shows TEM images of the individual blend components filled with MWNTs i.e. PC/CNT0.75, SAN/CNT0.75, and ABS/CNT0.75 samples. Within PC as matrix, the nanotubes are well dispersed and seen in most cases as single tubes. Moreover, they have a homogeneous distribution.

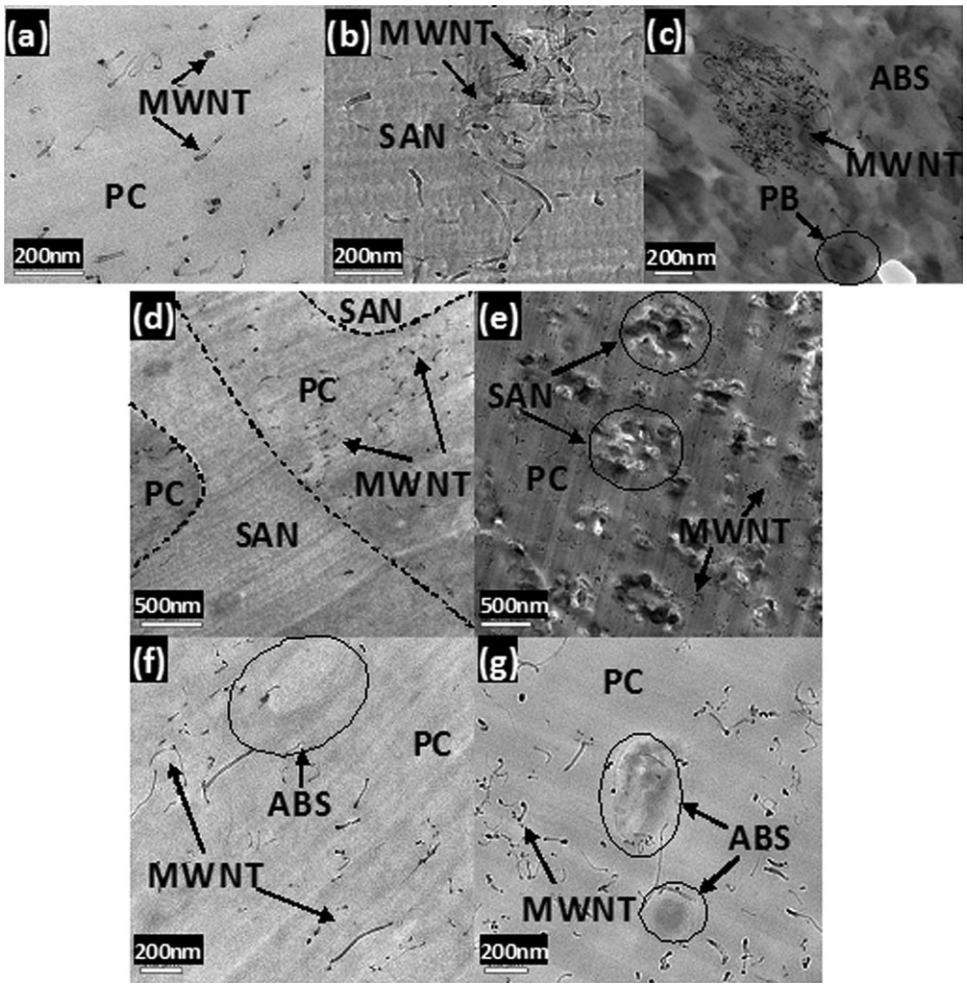

Figure 2. TEM images of MWNT-filled blend components and blend-based nanocomposites: (a) PC/CNT0.75, (b) SAN/CNT0.75, (c) ABS/CNT0.75, (d,e) PC70/SAN30/SANMA0.75/CNT0.75 and (f,g) PC70/ABS30/SANMA0.75/CNT0.75.

Generally, it is observed from Figure 2 that the state of nanotube dispersion is better within PC than those of SAN and ABS matrices. In SAN matrix, the nanotubes show areas with higher nanotube concentrations, indicating a worse state of dispersion and distribution. In ABS matrix, an enrichment of nanotubes in some areas is observed, which indicates nanotubes attraction toward the rubbery polybutadiene particles with sizes of about 200 nm. The attraction of nano-particles toward the rubbery polybutadiene fraction of ABS has been reported, earlier.[24]

To study the dispersion state of MWNTs in the blends and to determine the differences between performance of SAN and ABS in their blends with PC, two series of PC/SAN and PC/ABS blends (PC-rich, i.e., 70/30 for both the systems) were prepared, and their morphologies were investigated by TEM. The TEM results presented in Figure 2 clearly show that there is a kind of selective localization of MWNTs within one phase in both the systems. A disperse-matrix morphology, with PC as continuous phase, is seen for PC/ABS system, whereas the PC/SAN system shows a co-continuous morphology. In the case of PC/SAN system [Figure 2(d,e)], selective localization of MWNTs in PC phase can be concluded from comparing the areas of nanotube-free and nanotube-containing regions of TEM images. The result correlates with the studied volume blend composition that is about PC/ABS = 67/33 vol %. On the other hand, according to previous studies, the darker phase in TEM images of this blend can be assigned to PC phase.[11,25] This selective localization was attributed to lower interfacial energies between MWNTs and PC phase as compared to the SAN phase.[11] In case of the PC/ABS system [Figure 2(f,g)], a similar selective localization of MWNTs within the continuous PC phase is observed. However, small part of MWNTs is also located at the rubbery polybutadiene fraction of ABS.

Melt Rheological Properties

Next to morphological investigations, melt rheological characterization gives information about the structure of nanocomposites and blends. In addition, conclusions can be drawn toward the processing behavior of the nanocomposite blends. Therefore, frequency sweeps were performed on the materials. Complex viscosity, storage modulus, and loss modulus are shown in Figure 3(a,b), for T45 and T85 blends and the nanocomposites based on these blends, respectively. Generally, in all PC/ABS blends a non-Newtonian behavior is observed, which indicates existence of a yield stress phenomenon. Such behavior can be attributed to the rubbery polybutadiene fraction of the ABS

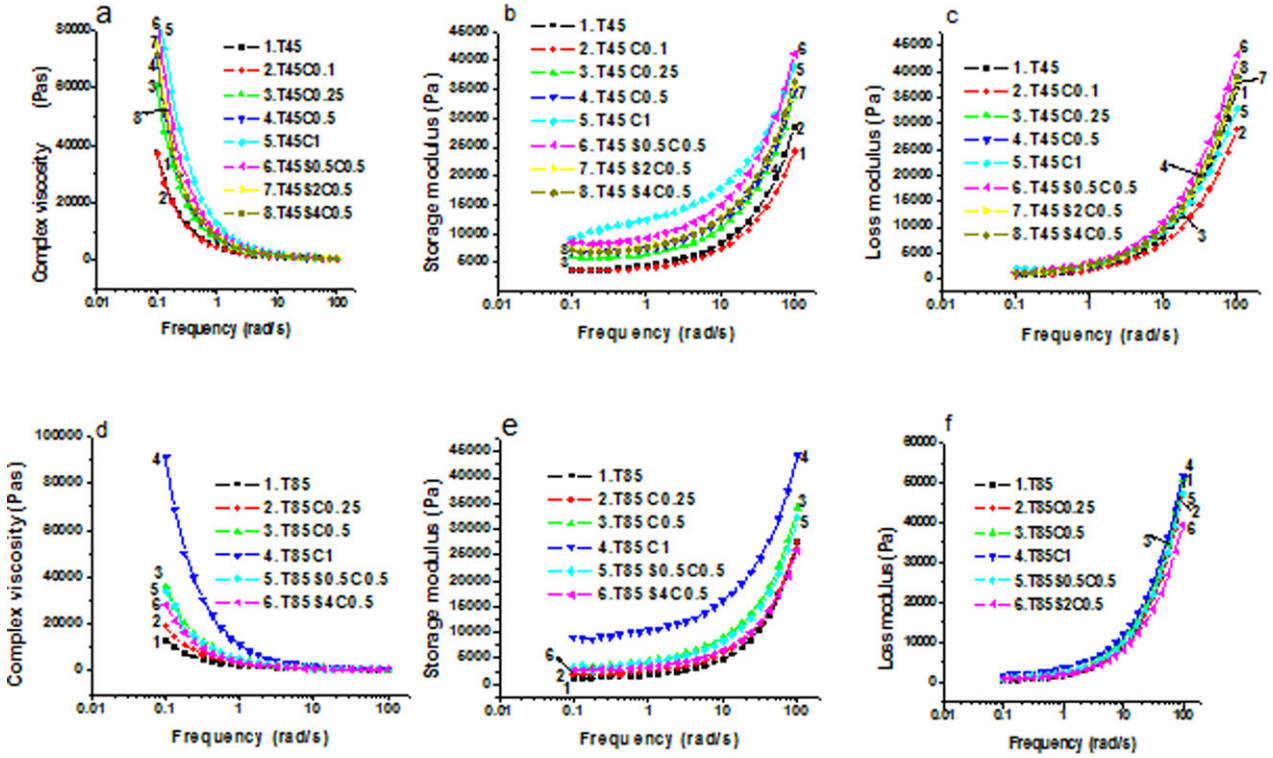

Figure 3. Rheological behavior of: T45 blend and the blend-based nanocomposites (a) complex viscosity, (b) shear storage modulus, (c) shear loss modulus; and T85 blend and the blend-based nanocomposites (d) complex viscosity, (e) shear storage modulus, (f) shear loss modulus. [Color figure can be viewed in the online issue, which is available at wileyonlinelibrary.com.]

component in the blends and nanocomposites.[26,27] Significant increase of viscosity with incorporation of MWNTs is seen, especially at low frequencies. The rheological behavior of the blends depends on the behavior of the blend components as well as on the blend morphology. Incorporation of CNT into the blends changes both the viscosity of filled (PC) phase and, as it was seen in the SEM investigations, the phase domain size. Therefore, the observed changes in rheological behavior should be attributed to the combined effect of these two phenomena, along with the nanotube-polymer network formation. Complex viscosity curve of nanocomposites incorporated with low amount of MWNTs (i.e., less than 0.25 wt % MWNTs) show a frequency dependency, similar to that of the neat blends. The addition of higher amounts of MWNT increases both storage and loss modulus, especially at low frequency region, whereas the effect on storage modulus is more significant as compared to that of loss modulus.

Incorporation of MWNTs to the neat blends in presence of an equal amount of SAN-MA causes insignificant decrease of complex viscosity and storage modulus at low frequencies, compared to the MWNTs-filled noncompatibilized sample (i.e., T85C0.5). This can be attributed to the inherent low complex viscosity and storage modulus of the compatibilizer, as compared to those of the blend components. A higher amount of SAN-MA results in a more significant decrease of the rheological characteristics.

Comparison between rheological response of T45 and T85 blends and their nanocomposites shows that T45-based samples have higher complex viscosity and storage modulus at terminal zone, compared to T85. This can be attributed to the higher ABS content of the T45 blend and its co-continuous morphology. ABS has generally a higher viscosity than PC due to presence of the rubbery PB fraction.

Electrical Properties

In context with the blend morphology, also changes in the electrical properties may be assumed. Figure 4(a,b) show the effect of MWNT contents up to 1 wt % on the electrical volume resistivity of T45- and T85-based nanocomposites, respectively.

The electrical resistivity of pure PC/ABS blend is ca. $2 \times 10^{+17}\ \Omega\ \mathrm{cm}^{-1}$, but addition of MWNT steeply decreases the electrical resistivity of the T45 and T85-based nanocomposites at 0.25 and 0.5 wt % MWNT, respectively. The observed steep decrease in electrical resistivity illustrates the formation of a continuous nanotubes conductive electrical path, and can be attributed to the electrical percolation threshold composition. Above these concentrations, the electrical resistivity decreases with increasing MWNTs content, gradually. The lower percolation threshold in T45 blends as compared to T85 can be explained with the morphology of these systems, which will be discussed, subsequently.

The addition of SAN-MA slightly decreases the electrical volume resistivity of T45 and T85 blend nanocomposites containing 0.5 wt % MWNT. This can be attributed to the observed changes in morphology, and formation of a more perfect co-continuous structure, as revealed by SEM analysis. It is observed that increase of SAN-MA/MWNTs weight ratio from 1 to 8 increases

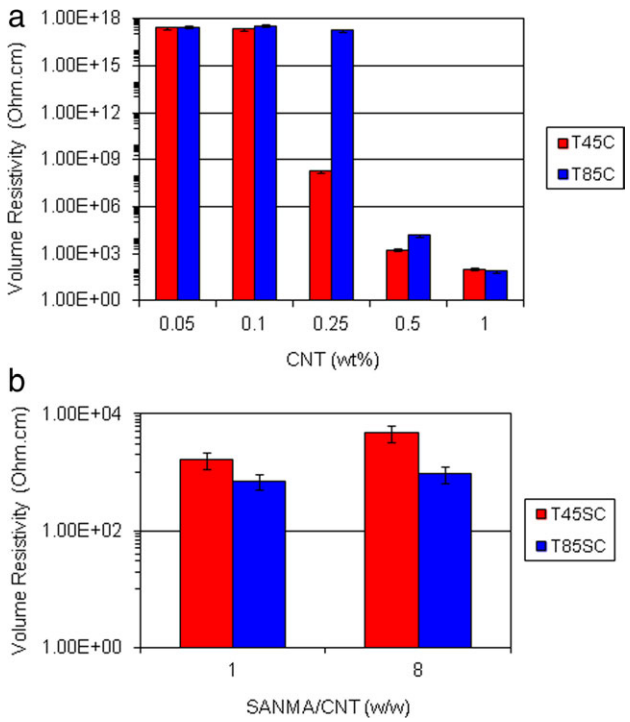

Figure 4. Electrical resistivity values of T45- and T85 blend-based nanocomposite containing: (a) different MWNTs, and (b) different SANMA/MWNT ratios. [Color figure can be viewed in the online issue, which is available at wileyonlinelibrary.com.]

the electrical resistivity [Figure 4(c,d)], attributed to role of compatibilizer in directing a part of MWNT from PC matrix toward ABS phase. Comparison between electrical resistivity values for compatibilized nanocomposites based on T45 and T85 blends shows that at a constant SAN-MA/MWNTs weight ratio, the electrical resistivity of compatibilized nanocomposites based on T85 blend is lower than that of sample based on T45 blend.

Correlation Between Morphological and Rheological Properties

The phase inversion composition can be predicted, based on blend components viscosities. According to the empirical relationship proposed by Avgeropoulos et al.[28] and its generalized format suggested by Paul and Barlow,[29] the phase inversion takes place when the volume ratio is equal to the viscosity ratio of the blend components. In the case of PC/ABS blend system the relationship can be expressed as follows:

$$\varphi_{ABS} = 1/(1 + \eta_{PC}/\eta_{ABS}) \quad (1)$$

where η and ϕ designate viscosity and volume fraction of blend components, respectively.

The model suggested by Utracki[30,31] incorporates intrinsic viscosity ($[\eta]$), as well. For the PC/ABS blend system it leads to the following expression:

$$\varphi_{ABS} = (1 - \log(\eta_{PC}/\eta_{ABS})/[\eta])/2 \quad (2)$$

where $[\eta]$ was assumed to be 1.9 for spherical domains.

Metelkin and Blekht[32] developed another approach, according to the theory of Tomotika[33] on instability of a liquid film/cylinder in another liquid. The expression adapted to the PC/ABS blend system can be written as:

$$\varphi_{ABS} = 1/(1 + F(\eta_{PC}/\eta_{ABS}) \times \eta_{PC}/\eta_{ABS}) \quad (3)$$

where F is obtained from the following equation:[31]

$$F(\eta_{PC}/\eta_{ABS}) = 1 + 2.25\ \log(\eta_{PC}/\eta_{ABS}) + 1.81[\log(\eta_{PC}/\eta_{ABS})]^2 \quad (4)$$

The predicted phase inversion composition according to the above three models are shown in Figure 5. The viscosity ratios were calculated from PC, ABS, PC/CNT0.75, and ABS/CNT0.75 complex viscosity values measured at the same frequencies. The dispersed phase volume percentage (ϕ_d%) was calculated from dispersed phase weight percentage using mixture's rule, with considering the densities of PC, and ABS as 1.20 and 1.04 g/cm^3, respectively. Some other relationships were also proposed by Ho et al.,[34] Kitayama and Keskkula,[35] and Everaert et al.[36] by modifying eq. (1), with introduction of some prefactors or exponents to achieve better fitting to the experimental data.

As observed in Figure 5, the Metelkin–Blekht equation shows that T45 blend (ABS-rich blend whose viscosity ratio was measured at 0.1 rad/s frequency) is close to the phase inversion region, while T85 blend (PC-rich blend whose viscosity ratio was measured at 0.1 rad/s frequency) has a dispersed-matrix type structure, which agrees well with the SEM observation discussed previously. Incorporation of 0.5 wt % MWNT into T45 blend puts it far from the phase inversion region, supporting the aforementioned SEM analysis. Tendency to the dispersed-matrix morphology with introduction of 0.5 wt % MWNT is also observed for T85 blend.

Correlation Between Electrical and Morphological Properties

Comparison between electrical resistivity values for nanocomposites shows that at a constant MWNTs content, the electrical

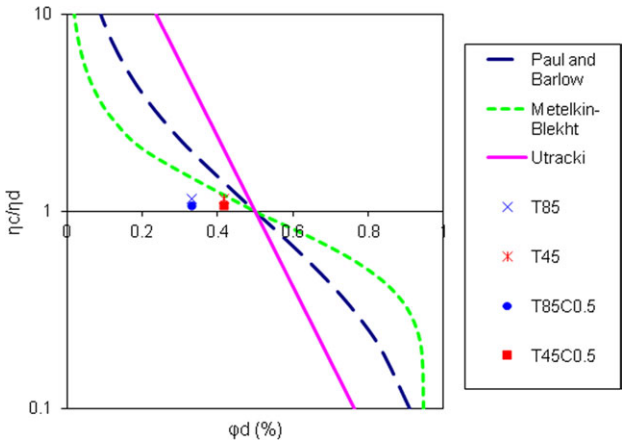

Figure 5. Phase inversion composition for PC/ABS blends and PC/ABS/MWNT nanocomposites according to Paul and Barlow, Metelkin Blekht, and Utracki models. [Color figure can be viewed in the online issue, which is available at wileyonlinelibrary.com.]

Applied Polymer SCIENCE

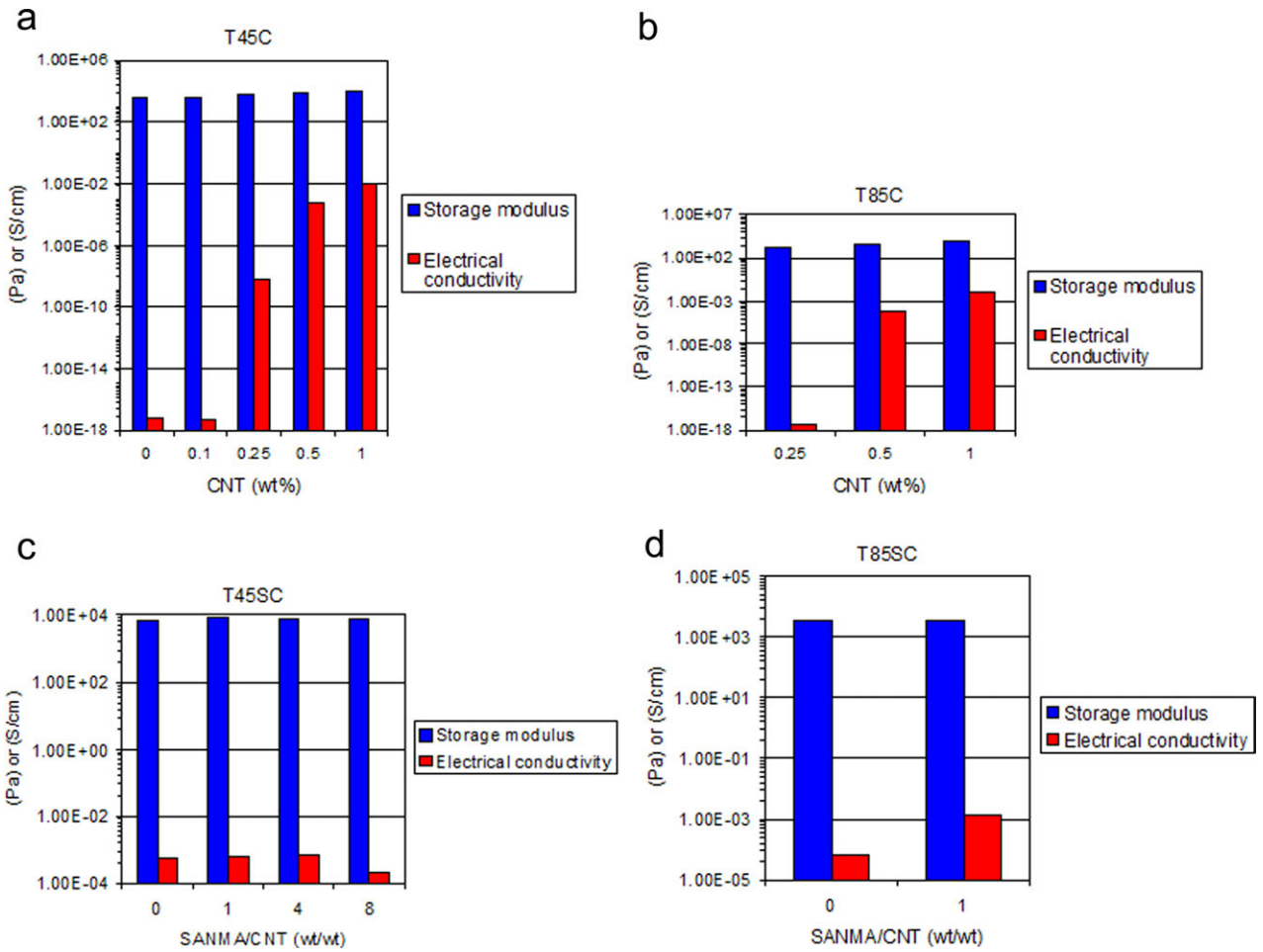

Figure 6. Correlation between electrical and rheological properties: (a) T45 containing different MWNT amounts, (b) T85 containing different MWNT amounts, (c) T45 containing different SANMA/MWNT ratios, and (d) T85 containing different SANMA/MWNT ratios. [Color figure can be viewed in the online issue, which is available at wileyonlinelibrary.com.]

resistivity of nanocomposites based on T85 blend is higher than those of T45 blend. Considering the fact that majority of MWNTs are localized in PC phase, in T45 blend-based nanocomposites having ABS-rich composition, MWNTs are localized in a lower content of PC, that is, 45 wt %, compared to T85 blend-based nanocomposites with higher PC content of 70 wt %, thus having a higher concentration in PC. Both the CNTs-filled T45 and T85 nanocomposite systems are considered double percolated systems. In the case of T45, the double percolation is attributed to its co-continuous structure, whereas the double percolation for T85 system occurs since PC phase, which accommodates all CNTs, is the blend matrix here.

Correlation Between Electrical and Rheological Characteristics

Figure 6(a,b) depict change of electrical conductivity (reciprocal to electrical volume resistivity) and storage modulus (values at 0.1 rad/s) versus CNT content and/or compatibilizer/CNT ratios, for T45 and T85 systems, respectively. The measured values of storage modulus and electrical conductivity increase monotonically with MWNT content. Comparing both qualities, the relative increase of these parameters is higher for electrical conductivity values than storage modulus. It is well known that electrical conductivity follows a percolation rule with a sharp change from the insulating polymer to a nanotube network, where the nanotubes may be wrapped by (insulating) polymer chains. This change has been reported to be in the range of 6–17 decades. In this study, the observed change in electrical conductivity is about 10 decades at the percolation thresholds (T45/CNT0.25 and T85/CNT0.5). In contrast, the storage modulus, representing the viscoelastic behavior in the melt state, changes up to 4 decades. The possible reason is that σ_{DC} is only affected by MWNTs-MWNTs network, while storage modulus is influenced by three kinds of networks, that is, polymer-polymer, polymer-MWNT and MWNT-MWNT. The changes in both conductivity and storage modulus with addition of compatibilizer is attributed to improved MWNTs dispersion state, due to its good interaction with SAN-MA within conductive phase, that is, PC.

CONCLUSIONS

Different amounts of MWNTs were added to commercial PC/ABS blends, co-continuous T45 (ABS-rich), and dispersed-type

T85 (PC-rich), in order to improve the blend properties. The changes in blend morphology, rheology, and electrical properties were studied in terms of variations in MWNT content, presence or absence of compatibilizer and compatibilizer/MWNTs ratio. Moreover, a PC/SAN/MWNT system with similar composition to that of T85 was made to define the role of polybutadiene fraction of the ABS component on dispersion state of MWNTs in the nanocomposites.

TEM results confirmed that in both the systems (T45 and T85) MWNT was mainly localized in PC phase of the blends. Addition of MWNTs to these blend systems led to significant enhancement of electrical conductivity of the blends. The electrical percolation threshold in the system with co-continuous morphology, due to double percolation phenomenon, was lower than that of the system with dispersed-type morphology. Moreover, incorporation of MWNT to these systems refined the blend morphologies. This refinement was attributed to localization of MWNT in PC matrix, which increased its elasticity and viscosity, and resulted in more viscous shear stresses being imposed on the ABS dispersed phase. The rheological percolation, in a similar manner to the electrical percolation, occurred at a lower MWNT content in the system with co-continuous morphology, as compared to that of the system with dispersed-type morphology. This reconfirmed the importance of double percolation phenomena.

SEM investigation and theoretical analysis using different models for prediction of the type of blend morphology for the both systems, in presence and absence of MWNT, confirmed that the type of morphology did not change by incorporation of MWNT into the blends.

A typical role of compatibilizer in refining blend morphology was observed in both systems. In addition, for T45 system, it changed the co-continuous morphology to dispersed-type, attributed to the viscosity reduction due to inherent low viscosity of the compatibilizer. With incorporation of MWNT in presence of compatibilizer to the T45 system, the morphology changed again to the co-continuous type but showed a more refined morphology. This refinement was in agreement with the findings on localization of MWNT in PC phase, and its consequences on blend rheological properties. The electrical conductivity of both the systems, filled with MWNT in presence of compatibilizer, was lower than the systems filled with MWNT only, attributed to role of compatibilizer in directing a part of MWNT from PC matrix toward ABS phase.

With increasing compatibilizer/MWNTs ratio, the influence of compatibilizer on refining morphology and reducing electrical conductivity was more pronounced. Because of inherent low viscosity of compatibilizer, its incorporation to both the systems decreased the viscosity. This reduction was such that it masked the viscosity and elasticity enhancement caused by incorporation of MWNT to these blend systems.

TEM analysis of PC/SAN/MWNT and PC/ABS/MWNT systems revealed a similar selective localization of MWNT within the continuous PC phase in both the systems. However, a small portion of MWNTs was also located on polybutadiene rubber fraction of ABS.

REFERENCES

1. Tennent, H. G. (Hyperion Catalysis International Inc.). U.S. Patent 4, 663,230, May 5, **1987**.
2. Iijima, S. *Nature* **1991**, *354*, 56.
3. Kuchibhatla, S. V. N. T.; Karakoti, A. S.; Bera, D.; Seal, S. *Prog. Mater. Sci.* **2007**, *52*, 699.
4. Meincke, O.; Kaempfer, D.; Weickmann, H.; Friedrich, C.; Vathauerb, M.; Warth, H. *Polymer* **2004**, *45*, 739.
5. Pötschke, P.; Bhattacharyya, A. R.; Janke, A. *Polymer* **2003**, *44*, 8061.
6. Pötschke, P.; Bhattacharyya, A. R.; Janke A. *Carbon* **2004**, *42*, 965.
7. Wu, M.; Shaw, L. *J. Appl. Polym. Sci.* **2006**, *99*, 477.
8. Pötschke, P.; Kretzschmar, B.; Janke, A. *Compos. Sci. Technol.* **2007**, *67*, 855.
9. Pötschke, P.; Pegel, S.; Claes, M.; Bonduel, D. *Macromol. Rapid. Commun.* **2008**, *29*, 244.
10. Fenouillot, F.; Cassagnau, P.; Majeste, J. C. *Polymer* **2009**, *50*, 1333.
11. Göldel, A.; Kasaliwal, G.; Pötschke, P. *Macromol. Rapid Commun.* **2009**, *30*, 423.
12. Wu, D. Z. Y.; Zhang, M.; Yu, W. *Biomacromolecules* **2009**, *10*, 417.
13. Balberg, I.; Anderson, C. H.; Alexander, S.; Wagner, N. *Phys. Rev. B* **1984**, *30*, 3933.
14. Wu, S. H.; Masaharu, I.; Natsuki, T.; Ni, Q. Q. *J. Reinf. Plast. Compos.* **2006**, *25*, 1957.
15. Pötschke, P.; Paul, D. R. *Macromol. Symp.* **2003**, *198*, 69.
16. Mutel, A. T.; Kamal, M. R. In Two Phase Polymer Systems; Utracki L. A.; Ed.; Carl Hanser:Munich, **1991**; p 305.
17. Abdel-Goad, M.; Pötschke, P. *J. Non-Newtonian Fluid Mech.* **2005**, *128*, 2.
18. Bhattacharyya, A. R.; Pötschke, P.; Abdel-Goad, M.; Fischer, D. *Chem. Phys. Lett.* **2004**, *392*, 28.
19. Pötschke, P.; Fornes, T. D.; Paul, D. R. *Polymer* **2002**, *43*, 3247.
20. Lin, B.; Sundararaj, U.; Pötschke, P. *Macromol. Mater. Eng.* **2006**, *291*, 227.
21. Pötschke, P.; Abdel-Goad, M.; Alig, I.; Dudkin, S.; Lellinger, D. *Polymer* **2005**, *45*, 8863.
22. Jin, S. H.; Choi, D. K.; Lee, D. S. *Colloids Surf. A* **2008**, *313*, 242.
23. Utracki, L. A. Polymer Alloys and Blends, Hanser: Munich, **1989**; p 128.
24. As'habi, L.; Jafari, S. H.; Baghaei, B.; Khonakdar, H. A.; Pötschke P.; Böhme F. *Polymer* **2008**, *49*, 2119.
25. Lednický, F.; Hromádková, J.; Kolarík, J. *Polym. Test.* **1999**, *18*, 123.
26. Jafari, S. H.; Pötschke, P.; Stephan, M.; Warth, H.; Alberts, H. *Polymer* **2002**, *43*, 6985.
27. Cui, L.; Zhou, Z.; Zhang, Y.; Zhang, Y.; Zhang, X.; Zhou, W. *J. Appl. Polym. Sci.* **2007**, *106*, 811.

28. Avgeropoulos, G. N.; Weissert, F. C.; Biddison, P. H.; Böhm, G. G. A. *Rubber Chem. Technol.* **1976**, *49*, 93.
29. Paul, D. R.; Barlow, J. W. *J. Macromol. Sci. Rev. Macromol. Chem.* **1980**, *C18 1*, 109.
30. Utracki, L. A. *J. Rheol.* **1991**, *35*, 1615.
31. Utracki, L. A. *Polym. Mater. Sci. Eng.* **1991**, *65*, 50.
32. Metelkin, V. I.; Blekht, V. P. *Colloid J. USSR* **1984**, *46*, 425.
33. Tomotika, S. *Proc. R. Soc. Lond. Ser. A* **1935**, *150*, 322.
34. Ho, R. M.; Wu, C. H.; Su, A. C. *Polym. Eng. Sci.* **1990**, *30*, 511.
35. Kitayama, N.; Keskkula, H.; Paul, D. R. *Polymer* **2000**, *41*, 8041.
36. Everaert, V.; Aerts, L.; Groeninckx, G. *Polymer* **1999**, *40*, 6627.